Modelling the vertical profiles of O2 and pH in saturated freshwater sediments

V. Devallois, P. Boyer, J.L. Boudenne, B. Coulomb

Ann. Limnol. - Int. J. Lim. 2008, 44 (4), 275-288

Modelling the vertical profiles of O_2 and pH in saturated freshwater sediments

V. Devallois [1,2], P. Boyer[1], J.L. Boudenne[2], B. Coulomb[2]

[1]IRSN/DEI/SECRE/Laboratoire de Modélisation Environnementale, CE Cadarache, Bâtiment 159, 13115 Saint Paul lez Durance, France.
[2] Université d'Aix-Marseille I, II, III - CNRS, Laboratoire Chimie Provence – UMR6264, Equipe « Chimie de l'Environnement Continental », 3 place Victor Hugo, case 29, 13331 Marseille cedex 3, France

Sediment-water interactions play an important role in influencing the water quality of aquatic systems. Water quality management of freshwater systems needs to take into account this behaviour, which depends largely on early diagenetic processes that condition the physical and biogeochemical properties of the sediment. Among these processes, the redox transformations resulting from the oxidation of organic matter by the microbial activity have a major influence on the biogeochemical properties of sediments. In particular, these reactions condition the vertical profiles of nutrient concentrations, pH and metals along the sedimentary column. This paper presents a method which couples both experimental and modelling approaches in order to characterise and analyse the biogeochemistry of freshwater sediments. The modelling approach is based on a coupling between biogeochemical processes and interstitial diffusion. As pore water pH influences the behaviour of the biogeochemical species, we have extended these models to allow for the calculation of pH by taking into account the inventory of protons consumed or produced by different biogeochemical reactions. In parallel, an analytical protocol has been developed to obtain vertical distributions of the main physicochemical parameters in natural sediments cores. To illustrate this approach, we apply our method to sediments cores sampled in the Durance, a river in the south-east of France.

Keywords: freshwater sediments, early diagenesis, pH, modelling.

Introduction

Sediment-water interactions play an important role in influencing the water quality of aquatic systems. For example, sediments may act as a sink for nutrients or trace metals remaining stocked after deposition and may therefore pose a risk to surface water quality and ecosystem health if environmental changes lead to release these stocks (Forstner & Wittmann 1981). Water quality management of freshwater systems needs to take into account this behaviour, which depends largely on early diagenetic processes that condition the physical and biogeochemical properties of the sediment (deposition, erosion, consolidation, interstitial diffusion, bioturbation, remineralization of organic matter by bacterial activities). Of these processes, the redox transformations resulting from the oxidation of organic matter have a major influence on the biogeochemical properties of sediments.

* Corresponding author : E-mail : valerie.devallois@irsn.fr

Different redox reactions occur in succession from the sediment water interface to the deeper layers according to the Gibbs free energy of the different electron acceptors (Froelich et al. 1979): oxic respiration, denitrification, manganese hydroxide and iron hydroxide reduction, sulphate reduction, methanogenesis. These reactions influence physicochemical parameters such as pH, redox potential or dissolved oxygen, which decrease with increasing sediment depth. These transformations increase concentration gradients and consequently lead to increased diffusive flux along the sediment column and between the sediment and the water columns. As these diffusive fluxes may affect the biogeochemical and ecological functioning of the hydrosystems (Middelburg & Soetaert 2005), a quantitative understanding of the interactions and controls of sediment biogeochemistry is needed to determine the long term fate of nutrients and pollutants in aquatic sediments. To this end, reactive transport models have been developed (Berg et al. 2003, Berner 1980, Boudreau 1997, Soetaert et al. 1996, Tromp et al. 1995, Van Cappellen &

Article available at http://www.limnology-journal.org or http://dx.doi.org/10.1051/limn:2008011

Wang 1997, Wang & Van Cappellen 1996, Wijsman et al. 2002) to simulate the complex interplay of reactions and transport processes in sediments.

In this paper we present a method which couples both experimental and modelling approaches in order to characterise and analyse the biogeochemistry of freshwater sediments. The modelling approach is based on a coupling between biogeochemical processes (Wang & Van Cappellen 1996) and interstitial diffusion (Boudreau 1996a, Boudreau 1996b). As pore water pH influences the behaviour of the biogeochemical species (Sigg et al. 2001), we have extended the existing model to allow for the calculation of pH by taking into account the inventory of protons consumed or produced by different biogeochemical reactions. In parallel, an analytical protocol has been developed to obtain vertical distributions of the main physicochemical parameters in natural sediments cores. To illustrate this approach, we apply our method to sediments cores sampled in the Durance, a river in the south-east of France.

Table 1. Chemical species included in the model

Species	Particulate form (mol.g^{-1})	Dissolved form (mol.l^{-1})	Colloidal form (mol.l^{-1})
Ammonium ions		$[NH_4^+]_D$	
Calcite	$[Calcite]_P$		
Calcium ions		$[Ca^{2+}]_D$	
Carbonate ions		$[\Sigma CO_3]_D$	
Oxygen		$[O_2]_D$	
Iron		$[Fe^{2+}]_D$	
Iron carbonates	$[FeCO_3]_P$		
Iron monosulphide	$[FeS]_P(z,t)$		
Iron oxide	$[Fe(OH)_3]_P$		$[Fe(OH)_3]_C$
Manganese		$[Mn^{2+}]_D$	
Manganese carbonates	$[MnCO_3]_P$		
Manganese oxide	$[MnO_2]_P$		$[MnO_2]_C$
Nitrate		$[NO_3^-]_D$	
Organic matter	$[POM]_P$		
Phosphate ions		$[\Sigma PO_4]_D$	
Pyrite	$[FeS_2]_P$		
Sulphate		$[SO_4^{2-}]_D$	
Sulphide		$[\Sigma H_2S]_D$	

Modelling

The variables considered in the model are the concentrations of 18 chemical species considered in three potential phases (particulate (P), dissolved (D) and colloidal (C)) and in function of the depth (z) and the time (t) (Table 1), which depend on the early diagenesis processes and interstitial diffusion of their mobile phases. In this table, the sums of carbonates, phosphates, sulphides and ammonia are calculated from the contributions of their different dissolved ionic forms :

$$[\Sigma CO_3]_D(z,t) = [CO_2]_D(z,t) + [CO_3^{2-}]_D(z,t) + [HCO_3^-]_D(z,t)$$

$$[\Sigma H_2S]_D(z,t) = [H_2S]_D(z,t) + [HS^-]_D(z,t)$$

$$[\Sigma PO_4]_D(z,t) = [HPO_4^{2-}]_D(z,t) + [H_2PO_4^-]_D(z,t)$$

$$[\Sigma NH_3]_D(z,t) = [NH_3]_D(z,t) + [NH_4^+]_D(z,t)$$

For each species, the particulate phase includes the fraction of the species adsorbed onto solid particles (diameter > 0.45 µm), those that are incorporated into the sediment, as well as those precipitated. The modelling proposed in this paper is divided into three linked sub-models : 1) interstitial diffusion of dissolved and colloidal species, 2) biogeochemical reactions and 3) pH determination. These three sub-models are described in the next sections.

Interstitial diffusion

Interstitial diffusion generates spatial displacements along the sediment column of the colloidal and dissolved species composing pore water. The interstitial diffusion sub-model applied Fick's first law :

$$\frac{\partial C(z,t)}{\partial t} = \frac{\partial}{\partial z}\left(D_{Sed}(z) \cdot \frac{\partial C(z,t)}{\partial z} \right)$$

where $D_{Sed}(z)$ (m.s^{-2}) is the coefficient of interstitial diffusion of a dissolved substance in the sediment (Boudreau 1997, Boudreau 1999). As molecules must follow convoluted paths to circumvent the sediment particles, the values of this parameter are lower than those of $D_m(z)$, the coefficient of molecular diffusion of a solution in water. D_{sed} is related to D_m by the following relationship (Berner 1980) :

$$D_{sed}(z) = \frac{D_m(z)}{\theta(z)^2}$$

where θ(z), the sediment tortuosity is related to the sediment porosity n(z) by the following relationship (Boudreau 1997) :

$$\theta(z)^2 = 1 - \ln(n^2(z))$$

We determined porosity profiles by fitting Athy's relationship (Boudreau 1997) on our experimental data :

$$n(z) = n_\infty + (n_0 - n_\infty) \cdot e^{-\tau \cdot z}$$

where n_0 and n_∞ are the porosity at the sediment water interface and at infinite depth, respectively, and τ (cm^{-1}) is a coefficient of attenuation.

We consider that the coefficient of molecular diffusion is the same for all the mobile species, and for the purposes of this model we use the value reported by Boudreau $D_m = 5 \cdot 10^{-6}\ cm^2 \cdot sec^{-1}$ (Boudreau 1997, Boudreau, 1999).

Biogeochemical modelling

The biogeochemical modelling follows the approach developed by Wang & Van Cappellen (Van Capellen & Wang 1997, Wang & Van Cappellen 1996, Wijsman et al. 2002) and involves the primary and the secondary reactions resulting from the organic matter oxidation by micro-organisms present in the sediment. The primary reactions are aerobic respiration, denitrification, MnO_2 and $Fe(OH)_3$ reduction and sulphate reduction. The secondary reactions are the precipitation of carbonate and sulphide phases with dissolved Fe and Mn and the eventual re-oxidation by O_2. We have added into the previous models the processes of calcite precipitation/dissolution, which allows us to determine the pH of pore water (see next section).

We suppose that the particulate (P) and colloidal (C) forms of manganese and iron oxides have the same biogeochemical behaviours. Consequently, we directly determine the variations of their total concentrations (T) :

$$[Fe(OH)_3]_T(z,t) = [Fe(OH)_3]_C(z,t)\cdot n(z) + [Fe(OH)_3]_P(z,t)\cdot(1-n(z))\cdot\rho_{sed}$$

$$[MnO_2]_T(z,t) = [MnO_2]_C(z,t)\cdot n(z) + [MnO_2]_P(z,t)\cdot(1-n(z))\cdot\rho_{sed}$$

where n(z), the porosity and ρ_{sed} ($g.l^{-1}$), the sediment density were measured experimentally.

Equations

In contrast to the models based on the multi-G theory that involve several pools of organic matter characterized by different mineralization kinetics (Boudreau 1999, Soetaert et al. 1996, Wang & Van Cappellen 1996, Wijsman et al. 2002), we consider that there is only one pool of organic matter ($(CH_2O)_x(NH_3)_y(H_3PO_4)$) where the molar C/P and N/P ratios are given by the Redfield numbers (x = 106 and y = 16). The different pathways of mineralization are described by first-order kinetics, all controlled by the same rate constant (k_{Min}).

Table 2. Primary chemical reactions

1) Aerobic respiration (AR)
$POM + (x+2\cdot y)\cdot O_2 \rightarrow x\cdot\Sigma CO_3 + y\cdot NO_3^- + \Sigma PO_4 + \frac{3\cdot y}{2}\cdot H_2O$
2) Denitrification (DEN)
$POM + \frac{4\cdot x}{5}\cdot NO_3^- \rightarrow x\cdot\Sigma CO_3 + y\cdot NH_3 + \frac{2\cdot x}{5}\cdot N_2 + \Sigma PO_4 + \frac{2\cdot x}{5}\cdot H_2O$
3) Manganese oxide reduction (MOR)
$POM + 2\cdot x\cdot MnO_2 + 3\cdot x\cdot CO_2 + x\cdot H_2O \rightarrow 4\cdot x\cdot\Sigma CO_3 + 2\cdot x\cdot Mn^{2+} + y\cdot NH_3 + \Sigma PO_4$
4) Iron oxide reduction (IOR)
$POM + 4\cdot x\cdot Fe(OH)_3 + 7\cdot x\cdot CO_2 \rightarrow 4\cdot x\cdot\Sigma CO_3 + 4\cdot x\cdot Fe^{2+} + y\cdot NH_3 + \Sigma PO_4 + 3\cdot x\cdot H_2O$
5) Sulphate reduction (SR)
$POM + \frac{1}{2\cdot x}\cdot SO_4^{2-} \rightarrow x\cdot\Sigma CO_3 + \frac{x}{2}\cdot\Sigma H_2S + y\cdot NH_3 + \Sigma PO_4 + x\cdot H_2O$

Table 3. Secondary chemical reactions

6) Iron monosulphur precipitation (ISP): $Fe^{2+} + HS^- \leftrightarrow FeS + H^+$
7) $MnCO_3$ precipitation (MP): $Mn^{2+} + HCO_3^- \leftrightarrow MnCO_3 + H^+$
8) $FeCO_3$ precipitation (IP): $Fe^{2+} + HCO_3^- \leftrightarrow FeCO_3 + H^+$
9) Calcite precipitation/dissolution (CP): $HCO_3^- + Ca^{2+} \leftrightarrow CaCO_3 + H^+$
10) Pyrite precipitation (PP): $FeS + H_2S \leftrightarrow FeS_2 + H_2$
11) Nitrification (N): $NH_4^+ + O_2 \leftrightarrow NO_3^- + 2\cdot H^+ + H_2O$
12) Manganese oxidation (MO): $Mn^{2+} + 0{,}5\cdot O_2 + H_2O \leftrightarrow MnO_2 + 2\cdot H^+$
13) Iron oxidation (IO): $Fe^{2+} + 0{,}25\cdot O_2 + 2{,}5\cdot H_2O \leftrightarrow Fe(OH)_3 + 2\cdot H^+$
14) Sulphide oxidation (SO): $H_2S + 2\cdot O_2 \leftrightarrow SO_4^{2-} + 2\cdot H^+$

The model is constructed with the five primary and nine secondary chemical reactions (Wang & Van Cappellen 1996, Wijsman et al. 2002) presented in tables 2 and 3.

From these chemical reactions, the variations of the different species are given by:

- $\frac{d[POM]_P(z,t)}{dt} = -V_{AR}(z,t) - V_{DEN}(z,t) - V_{MOR}(z,t) - V_{IOR}(z,t) - V_{SR}(z,t)$
- $\frac{d[MnO_2]_T(z,t)}{dt} = -2x\cdot V_{MOR}(z,t) - V_{MO}(z,t)$
- $\frac{d[Fe(OH)_3]_T(z,t)}{dt} = -4x\cdot V_{IOR}(z,t) + V_{IO}(z,t)$
- $\frac{d[FeS]_P(z,t)}{dt} = V_{IMP}(z,t) - V_{PP}(z,t)$

- $\frac{d[FeS]_P(z,t)}{dt} = V_{IMP}(z,t) - V_{PP}(z,t)$

- $\frac{d[MnCO_3]_P(z,t)}{dt} = V_{MP}(z,t)$

- $\frac{d[FeCO_3]_P(z,t)}{dt} = V_{IP}(z,t)$

- $\frac{d[Calcite]_P(z,t)}{dt} = V_{CP}(z,t)$

- $\frac{d[Ca^{2+}]_D(z,t)}{dt} = -V_{CP}(z,t)$

- $\frac{d[NO_3^-]_D(z,t)}{dt} = y \cdot V_{AR}(z,t) - \frac{4}{5} x \cdot V_{DEN}(z,t) + V_N(z,t)$

- $\frac{d[SO_4^{2-}]_D(z,t)}{dt} = -\frac{1}{2} x \cdot V_{SR}(z,t) + V_{SO}(z,t)$

- $\frac{d[O_2]_D(z,t)}{dt} = -(x+2y) \cdot V_{AR}(z,t) - V_N(z,t) - V_{MO}(z,t) - V_{IO}(z,t) - V_{SO}(z,t)$

- $\frac{d[Mn^{2+}]_D(z,t)}{dt} = 2x \cdot V_{MOR}(z,t) - V_{MP}(z,t) - V_{MO}(z,t)$

- $\frac{d[Fe^{2+}]_D(z,t)}{dt} = 4x V_{IOR}(z,t) - V_{ISR}(z,t) - V_{IP}(z,t) - V_{IO}(z,t)$

- $\frac{d[\Sigma H_2S]_D(z,t)}{dt} = \frac{1}{2} x \cdot V_{SR}(z,t) - V_{ISR}(z,t) - V_{PP}(z,t) - V_{SO}(z,t)$

- $\frac{d[\Sigma PO_4]_D(z,t)}{dt} = V_{AR}(z,t) + V_{DEN}(z,t) + V_{MOR}(z,t) + V_{IOR}(z,t) + V_{SR}(z,t)$

- $\frac{d[\Sigma CO_3]_D(z,t)}{dt} = x \cdot V_{AR}(z,t) + x \cdot V_{DEN}(z,t) + x \cdot V_{MOR}(z,t) + x \cdot V_{IOR}(z,t) + \cdot$
$\cdot x \cdot V_{SR}(z,t) - V_{MP}(z,t) - V_{IP}(z,t) - V_{CP}(z,t)$

- $\frac{d[NH_4^+]_D(z,t)}{dt} = y \cdot V_{AR}(z,t) + y \cdot V_{DEN}(z,t) + y \cdot V_{MO}(z,t) + \ldots$
$y \cdot V_{SR}(z,t) - V_N(z,t)$

For the primary reactions, the reactions rates are described by a Michaelis-Menten kinetics based on a competition between a limitation term modelled by a Monod-type hyperbolic limitation function (Soetaert et al. 1996, Wijsman et al. 2002)and an inhibition term described by a reciprocal hyperbolic function (Soetaert et al. 2007, VanCappellen & Wang 1997, Wijsman 2001) :

$$V_R(z,t) = k_{Min} \cdot [POM](z,t) \cdot \underbrace{\frac{[EA](z,t)}{[EA](z,t) + k_{Li}^{EA}}}_{\text{limitation}} \cdot \underbrace{\prod_i \frac{k_{In,R}^{IN_i}}{[IN]_i(z,t) + k_{In,R}^{IN_i}}}_{\text{inhibition}}$$

with $\Delta G^0(N_i) > \Delta G^0(EA)$

where k_{Min}^{POM} (s^{-1}) is the rate constant of organic matter remineralization, [EA] ($mol.l^{-1}$) is the concentration of the electron acceptor, k_{Li}^{EA} ($mol.l^{-1}$) is the half-saturation concentration of EA that limits the reaction, $[IN]_i$ ($mol.l^{-1}$) are the concentrations of the inhibiting oxidants that have higher free energy ($\Delta G°$) than EA and $k_{In,R}^{N_i}$ ($mol.l^{-1}$) are the associated inhibition constants.

This equation represents the sequence of degradation pathways described by Froelich (1979) where the classification of the electron acceptors in the order of their free energy is : $\Delta G°(O_2) > \Delta G°(NO_3^-) > \Delta G°(MnO_2) > \Delta G°(Fe(OH)_3) > \Delta G°(SO_4^{2-})$.

The reactions rates of the five primary reactions are given by :

- $V_{AR}(z,t) = k_{Min} \cdot [POM]_p(z,t) \cdot \frac{[O_2]_D(z,t)}{[O_2]_D(z,t) + k_{Li}^{O_2}}$

- $V_{DEN}(z,t) = k_{Min} \cdot [POM]_p(z,t) \cdot \frac{[NO_3^-]_D(z,t)}{[NO_3^-]_D(z,t) + k_{Li}^{NO_3^-}} \cdot \frac{k_{In,DEN}^{O_2}}{[O_2]_D(z,t) + k_{In,DEN}^{O_2}}$

- $V_{MOR}(z,t) = k_{Min} \cdot [POM]_P(z,t) \cdot \frac{[MnO_2]_T(z,t)}{[MnO_2]_T(z,t) + k_{Li}^{MnO_2}} \cdot \frac{k_{In,MOR}^{O_2}}{[O_2]_D(z,t) + k_{In,MOR}^{O_2}} \cdot \frac{k_{In,MOR}^{NO_3^-}}{[NO_3^-]_D(z,t) + k_{In,MOR}^{NO_3^-}}$

- $V_{IOR}(z,t) = k_{Min} \cdot [POM]_P(z,t) \cdot \frac{[Fe(OH)_3]_T(z,t)}{[Fe(OH)_3]_T(z,t) + k_{Li}^{Fe(OH)_3}} \cdot \frac{k_{In,IOR}^{O_2}}{[O_2]_D(z,t) + k_{In,IOR}^{O_2}} \cdot \frac{k_{In,IOR}^{NO_3^-}}{[NO_3^-]_D(z,t) + k_{In}^{NO_3^-}} \cdot \frac{k_{In,IOR}^{MnO_2}}{[MnO_2]_T(z,t) + k_{In,IOR}^{MnO_2}}$

- $V_{SR}(z,t) = k_{Min} \cdot [POM]_P(z,t) \cdot \frac{[SO_4^{2-}]_D(z,t)}{[SO_4^{2-}]_D(z,t) + k_{Li}^{SO_4^{2-}}} \cdot \frac{k_{In,SR}^{O_2}}{[O_2]_D(z,t) + k_{In,SR}^{O_2}} \cdot \frac{k_{In,SR}^{NO_3^-}}{[NO_3^-]_D(z,t) + k_{In,SR}^{NO_3^-}} \cdot \frac{k_{In,SR}^{MnO_2}}{[MnO_2]_T(z,t) + k_{In,SR}^{MnO_2}} \cdot \frac{k_{In,SR}^{Fe(OH)_3}}{[Fe(OH^-)_3]_T(z,t) + k_{In,SR}^{Fe(OH)_3}}$

The secondary reactions involve re-oxidation and precipitation. The reaction rates for precipitation/dissolution reactions depend on the degree of saturation (Ω_R) of the pore water for the concerned species :

$$\Omega_R(z,t) = \frac{[A](z,t)\cdot[B](z,t)}{[H^+](z,t)\cdot Ks_{AB}}$$

where [A] and [B] (mol.l^{-1}) are the concentrations of the species concerned by the reaction, [H$^+$] (mol.l^{-1}) is the proton concentration and Ks_{AB} (mol.l^{-1}) is the apparent solubility product of the reaction.

If $\Omega_R(z,t) > 1$, the precipitation takes place at the rate: $V_R(z,t) = k^+_{AB}\cdot(\Omega_R(z,t)-1)$

If $\Omega_R(z,t) < 1$, the dissolution of AB takes place at the rate: $V_R(z,t) = k^-_{AB}\cdot[AB](z,t)\cdot(\Omega_R(z,t)-1)$
where k^+_{AB} and k^-_{AB} are the forward and backward first-order rate constants respectively.

- $$V_{ISP}(z,t) = \begin{cases} k^+_{ISP}\cdot(\Omega_{ISP}(z,t)-1) & if\ \Omega_{ISP}(z,t) > 1 \\ k^-_{ISP}\cdot[FeS](z,t)\cdot(\Omega_{SP}(z,t)-1) & if\ \Omega_{ISP}(z,t) < 1 \end{cases}$$

- $$V_{MP}(z,t) = \begin{cases} k^+_{MP}\cdot(\Omega_{MP}(z,t)-1) & if\ \Omega_{MP}(z,t) > 1 \\ k^-_{MP}\cdot[MnCO_3]\cdot(\Omega_{MP}(z,t)-1) & if\ \Omega_{MP}(z,t) < 1 \end{cases}$$

- $$V_{IP}(z,t) = \begin{cases} k^+_{IP}\cdot(\Omega_{IP}(z,t)-1) & if\ \Omega_{IP}(z,t) > 1 \\ k^-_{IP}\cdot[FeCO_3]\cdot(\Omega_{IP}(z,t)-1) & if\ \Omega_{IP}(z,t) < 1 \end{cases}$$

- $$V_{CP}(z,t) = \begin{cases} k^+_{CP}\cdot(\Omega_{CP}(z,t)-1) & if\ \Omega_{CP}(z,t) > 1 \\ k^-_{CP}\cdot[CaCO_3]\cdot(\Omega_{CP}(z,t)-1) & if\ \Omega_{CP}(z,t) < 1 \end{cases}$$

The formation of pyrite is described by bi-molecular rate kinetics (Rickard 1997, Rickard & Luther III 1997):
$V_{PP}(z,t) = k_{PP}\cdot[FeS](z,t)\cdot[H_2S](z,t)$
where k_{PP} (L.mol^{-1}.s^{-1}) is the first order rate constant of the reaction.

The reaction rates of the re-oxidation reactions are described by bi-molecular reaction rate laws (Wang & Van Cappellen 1996) :
$V_R(z,t) = k_R\cdot[EA](z,t)\cdot[ED](z,t)$
where V_R (mol.l^{-1}.s^{-1}) is the reaction rate, k_R (L.mol^{-1}.s^{-1}) is the reaction rate constant and [EA] and [ED] (mol.l^{-1}) are the concentrations of the electron acceptor and electron donor, respectively.

The reaction rates for the four re-oxidation reactions are :

- $V_N(z,t) = k_N\cdot[NH_4^+](z,t)\cdot[O_2](z,t)$
- $V_{MO}(z,t) = k_{MO}\cdot[Mn^{2+}](z,t)\cdot[O_2](z,t)$
- $V_{IO}(z,t) = k_{IO}\cdot[Fe^{2+}](z,t)\cdot[O_2](z,t)$
- $V_{SO}(z,t) = k_{SO}\cdot[H_2S](z,t)\cdot[O_2](z,t)$

Parameters

The values of the different parameters involved in these equations are obtained by fitting our model on analytical results (see experimental protocol section). Their relevance is evaluated by comparing our values to those found in the literature (Table 4).

pH modelling

pH determination requires proton concentrations [H$^+$] which depend on a complex set of reactions which control the acid-base properties of pore water (Jourabchi et al. 2005). In our model, pH is a calculated function and not a forced function as in other studies (Wijsman et al. 2001). Here, pH is calculated from the concentrations of the ionic species present in the pore water by considering :

1. the production and the consumption of protons by the biogeochemical reactions (Table 5) (Soetaert et al. 2007).

2. the following acid-base equilibria (Boudreau 1997) :

(c_1) $CO_2(aq) + H_2O \leftrightarrow HCO_3^- + H^+$
(c_2) $HCO_3^- \leftrightarrow CO_3^{2-} + H^+$
(s_1) $H_2S \leftrightarrow HS^- + H^+$
(s_2) $HS^- \leftrightarrow S^{2-} + H^+$
(p_1) $H_3PO_4 \leftrightarrow H_2PO_4^- + H^+$
(p_2) $H_2PO_4^- \leftrightarrow HPO_4^{2-} + H^+$
(p_3) $HPO_4^{2-} \leftrightarrow PO_4^{3-} + H^+$
(n) $NH_4^+ \leftrightarrow NH_3 + H^+$
(e) $H_2O \leftrightarrow OH^- + H^+$

These two points are linked by the mass conservation of the chemical species and the equation of electroneutrality.

We determine pH from the ionic concentrations provided by the previously described biogeochemical model in three successive steps: 1) resolution of the acid-base equilibria, 2) conservation of mass and 3) deduction of the proton concentration from the equation of electroneutrality. These three steps are described below.

Table 4. Bibliographic summary of biogeochemical parameter values

Parameters	Description	Values	References
k_{Min}	Organic matter mineralisation constant	8,7.10-7 - 3,5.10-8 s-1 8.10-10 - 9,5.10-7 s-1 9,4.10-8 s-1 3.10-9 s-1	(Wijsman 2001) (Wang & VanCappellen 1996) (Tromp et al. 1995) (Berg et al. 2003)
$k_{Li}^{O_2}$	Half-saturation concentration O2 limitation for oxic mineralisation	3.10-6 (mol.l-1) 3 - 20.10-6 (mol.l-1)	(Wijsman 2001) (Wang & VanCappellen 1996)
$k_{Li}^{NO_3^-}$	Half-saturation concentration NO3- limitation for denitrification	30.10-6 (mol.l-1) 4 – 80.10-6 (mol.l-1)	(Wijsman 2001) (Wang & VanCappellen 1996)
$k_{Li}^{MnO_2}$	Half-saturation concentration MnO2 limitation for manganese oxide reduction	5000.10-6 (mol.l-1) 4 - 32.10-6 (mol.l-1) 16. 10-6 (mol.l-1)	(Wijsman 2001) (Wang & VanCappellen 1996) (Canavan 2006)
$k_{Li}^{Fe(OH)_3}$	Half-saturation concentration Fe(OH)3 limitation for iron oxide reduction	12500.10-6 (mol.l-1) 200.10-6 (mol.l-1) 65-100.10-6 (mol.l-1)	(Wijsman 2001) (Canavan 2006) (Wang & VanCappellen 1996)
$k_{Li}^{SO_4^{2-}}$	Half-saturation concentration SO42- limitation for sulfate reduction	1620.10-6(mol.l-1) 100.10-6 (mol.l-1)	(Wijsman 2001) Jourabchi et al. 2005
$k_{In,D}^{O_2}$	Half-saturation concentration O2 inhibition constant for denitrification	10.10-6 (mol.l-1) 8.10-6 (mol.l-1) 1-30.10-6 (mol.l-1)	Soetaert et al. 1996 (Wijsman, 2001) (Wang and VanCappellen, 1996)
$k_{In,[MOR,IOR,SR]}^{O_2}$	Half-saturation concentration O2 inhibition for anoxic mineralisation	5.10-6 (mol.l-1) 3,1.10-6 (mol.l-1)	(Wijsman 2001) (Wang & VanCappellen 1996)
$k_{In}^{NO_3^-}$	Half-saturation concentration NO3- inhibition for anoxic mineralisation	10.10-6 (mol.l-1) 30.10-6 (mol.l-1)	(Wijsman 2001) (Wang & VanCappellen 1996)
$k_{In}^{MnO_2}$	Half-saturation concentration MnO2 inhibition for anoxic mineralisation	5000.10-6 (mol.l-1) 4 - 32.10-6 (mol.l-1)	(Wijsman 2001) (Wang & VanCappellen, 1996)
$k_{In}^{Fe(OH)_3}$	Half-saturation concentration Fe(OH)3 inhibition for anoxic mineralisation	12500.10-6 (mol.l-1) 200.10-6 (mol.l-1) 65-100.10-6 (mol.l-1)	(Wijsman 2001) (Canavan 2006) (Wang & VanCappellen 1996)
Ks_{FeS}	Apparent solubility product FeS	6310.10-6 (mol.l-1) 10-2,2 (mol.l-1)	(Rickard 2006) (Wang & VanCappellen 1996)
Ks_{MnCO_3}	Apparent solubility product MnCO3	100,193 (mol.l-1)	(Wang & VanCappellen 1996)
Ks_{FeCO_3}	Apparent solubility product FeCO3	100,192 (mol.l-1)	(Wang & VanCappellen 1996)
Ks_{CaCO_3}	Apparent solubility product CaCO3	10-1,99 (mol.l-1)	(Jahnke et al. 1997)
k_{ISP}^{+}	FeS précipitation rate constant	0,47 (l.mol-1.s-1) 11,5 (l.mol-1.s-1)	(Berg et al. 2003) (Wijsman et al. 2002)
k_{ISP}^{-}	FeS dissolution rate constant	3,15.10-11 (s-1) 3,2.10-11 (s-1)	(Rickard 2006) (Wijsman 2001)
k_{MP}^{+}	MnCO3 precipitation rate constant	2,1.10-11 (l.mol-1.s-1)	(Wang & VanCappellen 1996)
k_{MP}^{-}	MnCO3 dissolution rate constant	2,5.10-8 (s-1)	(Wang & VanCappellen 1996)
k_{IP}^{+}	FeCO3 precipitation rate constant	1,3.10-10 (l.mol -1.s-1)	(Wang & VanCappellen 1996)
k_{IP}^{-}	FeCO3 dissolution rate constant	1,6.10-8 (s-1)	(Wang & VanCappellen 1996)
k_{CP}^{+}	Calcite precipitation rate constant	0,5 - 6,4.10-8 (l.mol-1.s-1) 3,2.10-8 (l.mol-1.s-1)	(Adler et al. 2001, Jahnke et al. 1997) (Gutjahr et al. 1996a, Gutjahr et al. 1996b)

Parameters	Description	Values	References
k_{CP}^{-}	Calcite dissolution rate constant	0,14 - 30.10-8 (s-1) 1,5 - 3.10-10 (s-1)	(Gutjahr et al.1996b; Jahnke et al. 1997) (Adler et al. 2001)
k_{PP}	Pyrite formation rate constant	1,1.10-4 (l.mol-1.s-1)	(Rickard 1997; Rickard LutherIII 1997)
k_N	Nitrification rate constant	0,3 (l.mol-1.s-1) 0,7 (l.mol-1.s-1)	(Canavan 2006, Wijsman 2001) (Berg et al. 2003)
k_{MO}	Manganese oxidation rate constant	1,1.10-2 – 63 (l.mol-1.s-1)	(Berg et al. 2003, Canavan 2006)
k_{IO}	Iron oxidation rate constant	1,1.10-2 – 507 (l.mol-1.s-1)	(Berg et al. 2003, Canavan 2006)
k_{SO}	Sulphide oxidation rate constant	5.10-3 – 51 (l.mol-1.s-1)	(Berg et al. 2003, Canavan 2006)

Table 5. Influence of biogeochemical reactions on pH variations

Reactions	H+ ions variation	pH
Oxic respiration	Production	↓
Denitrification	Production	↓
Mn oxide reduction	Consumption	↑
Fe oxide reduction	Consumption	↑
Sulphate reduction	Production	↓
Precipitation of FeS	Production	↓
Precipitation of pyrite	Consumption	↑
Precipitation of MnCO3	Production	↓
Precipitation of FeCO3	Production	↓
Re-oxidation by O2	Production	↓
Dissolution of calcite	Consumption	↑

Acid-base equilibria

The acid-base reactions are characterized by their equilibrium constants (Sigg et al. 2001) :

• Carbonate acid-base equilibria

$$Kc_1 = \frac{[H^+](z,t)\cdot[HCO_3^-](z,t)}{[CO_2](z,t)} = 10^{-6,4}\ ;$$

$$Kc_2 = \frac{[H^+](z,t)\cdot[CO_3^{2-}](z,t)}{[HCO_3^-](z,t)} = 10^{-10,3}$$

• Sulphur acid-base equilibria

$$Ks_1 = \frac{[H^+](z,t)\cdot[HS^-](z,t)}{[H_2S](z,t)} = 10^{-7}\ ;$$

$$Ks_2 = \frac{[H^+](z,t)\cdot[S^{2-}](z,t)}{[HS^-](z,t)} = 10^{-13}$$

• Phosphate acid-base equilibria

$$Kp_1 = \frac{[H^+](z,t)\cdot[H_2PO_4^-](z,t)}{[H_3PO_4](z,t)} = 10^{-2,15}\ ;$$

$$Kp_2 = \frac{[H^+](z,t)\cdot[HPO_4^{2-}](z,t)}{[H_2PO_4^-](z,t)} = 10^{-7,2}$$

• Ammonia acid-base equilibrium:

$$K_N = \frac{[H^+](z,t)\cdot[NH_3](z,t)}{[NH_4^+](z,t)} = 10^{-7}$$

• Hydrolysis:

$$K_e = [H^+](z,t)\cdot[OH^-](z,t) = 10^{-14}$$

The pH of pore water in freshwater sediments generally ranges from 6 to 9. Consequently, the equilibria (s_2, p_1 et p_3) were not considered because the concentrations of the concerned species (S^{2-}, H_3PO_4, PO_4^{3-} respectively) are negligible in the relevant pH range.

Mass conservation

The acid-base equilibria introduce the different ionic forms of carbonates, phosphates, sulphurs and ammonia while the biogeochemical modelling resolves the total concentrations of these species without taking into account their speciation. This speciation is then determined by combining acid-base equilibria and the mass conservation of these four species :

$$[\Sigma CO_3]_D(z,t) = [CO_2]_D(z,t) + [CO_3^{2-}]_D(z,t) + [HCO_3^-]_D(z,t)$$

$$[\Sigma H_2S]_D(z,t) = [H_2S]_D(z,t) + [HS^-]_D(z,t)$$

$$[\Sigma PO_4]_D(z,t) = [HPO_4^{2-}]_D(z,t) + [H_2PO_4^-]_D(z,t)$$

$$[\Sigma NH_3]_D(z,t) = [NH_3]_D(z,t) + [NH_4^+]_D(z,t)$$

It is now possible to write the ionic concentrations of these four species in function of their total concentrations (previously calculated) and of the proton concentration.

$$[HCO_3^-]_D(z,t) = \frac{[H^+]_D(z,t)\cdot Kc_1}{[H^+]_D^2(z,t) + [H^+]_D(z,t)\cdot Kc_1 + Kc_1\cdot Kc_2}\cdot [\Sigma CO_3]_D(z,t)$$

$$[CO_2]_D(z,t) = \frac{[H^+]_D{}^2(z,t)}{[H^+]_D{}^2(z,t) + Kc_1\cdot[H^+]_D(z,t) + Kc_1\cdot Kc_2}\cdot [\Sigma CO_3]_D(z,t)$$

$$[CO_3^{2-}]_D(z,t) = \frac{Kc_1\cdot Kc_2}{[H^+]_D{}^2(z,t) + Kc_1\cdot[H^+]_D(z,t) + Kc_1\cdot Kc_2}\cdot [\Sigma CO_3]_D(z,t)$$

$$[H_2S]_D(z,t) = \frac{[H^+]_D(z,t)}{[H^+]_D(z,t) + Ks_1}\cdot[\Sigma H_2S]_D(z,t)$$

$$[HS^-]_D(z,t) = \frac{Ks_1}{[H^+]_D(z,t) + Ks_1}\cdot[\Sigma H_2S]_D(z,t)$$

$$[H_2PO_4^-]_D(z,t) = \frac{[H^+]_D(z,t)}{[H^+]_D(z,t) + Kp_2}\cdot[\Sigma PO_4]_D(z,t)$$

$$[HPO_4^{2-}]_D(z,t) = \frac{Kp_2}{[H^+]_D(z,t) + Kp_2}\cdot[\Sigma PO_4]_D(z,t)$$

$$[NH_4^+]_D(z,t) = \frac{[H^+]_D(z,t)}{[H^+]_D(z,t) + K_N}\cdot[\Sigma NH_3]_D(z,t)$$

$$[NH_3]_D(z,t) = \frac{K_N}{[H^+]_D(z,t) + K_N}\cdot[\Sigma NH_3]_D(z,t)$$

Equation of electroneutrality

Finally, the concentration of protons in pore water is determined by introducing the previous equations into the electroneutrality equation: $\Sigma[\text{ions}^+] = \Sigma[\text{ions}^-]$. By writing this equation in function of all ions modelled in pore water, the proton concentration becomes the only unknown :

$$[H^+]_D(z,t) = \left\{ \begin{array}{l} \dfrac{Kc_1\cdot(2\cdot Kc_2 + [H^+]_D(z,t))}{[H^+]_D{}^2(z,t) + Kc_1\cdot[H^+]_D(z,t) + Kc_1\cdot Kc_2}\cdot[\Sigma CO_3]_D(z,t) + \dfrac{Ks_1}{[H^+]_D(z,t) + Ks_1}\cdot[\Sigma H_2S]_D(z,t) \\ + \dfrac{[H^+]_D(z,t) + 2\cdot Kp_2}{[H^+]_D(z,t) + Kp_2}\cdot[\Sigma PO_4]_D(z,t) + [Cl^-]_D(z,t) \\ + \dfrac{Ke}{[H^+]_D(z,t)} + [NO_3^-]_D(z,t) + 2\cdot[SO_4^{2-}]_D(z,t) \\ - \dfrac{[H^+]_D(z,t)}{[H^+]_D(z,t) + K_N}\cdot[\Sigma NH_3]_D(z,t) \\ - 2\cdot[Ca^{2+}]_D(z,t) - 2\cdot[Fe^{2+}]_D(z,t) - 2\cdot[Mn^{2+}]_D(z,t) \end{array} \right.$$

Method of resolution

The resolution is performed with a one dimensional finite difference method based on an explicit numerical scheme. The sediment core is represented by a vertical column of height h (m), which is represented by Ndz (= h/Δz) discrete elementary layers having a thickness Δz (m) (Fig. 1). The simulated period T is represented by Ndt (= T/Δt) time steps Δt. From these considerations, a variable A, associated to the layer idz at the time iteration idt is noted: A_{idz}^{idt} . For all species (P, D and C), the domain is initialized by the conditions A_{idz}^{0} and the first section is associated to the limit conditions defined by A_0^{idt} . The interstitial diffusion model is resolved first. The intermediate solutions, noted *, are used for the resolution of the biogeochemical modelling. After this last step, the vertical distribution of pH is calculated.

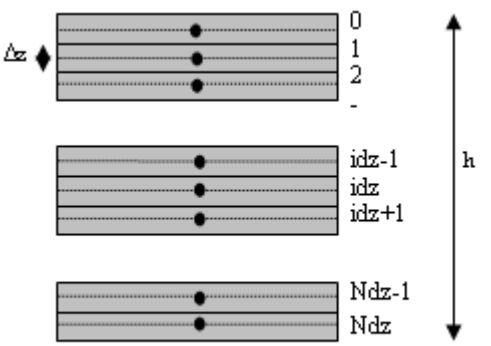

Fig.1. Discrete elementary layers of a sediment column

Resolution of the interstitial diffusion model

The equation of diffusion is resolved for each mobile phase (dissolved and colloidal) with a numerical method based on the following explicit finite differences scheme (Fig. 2) :

$$[C]_{idz}^{idt^*} = a \cdot [C]_{idz-1}^{idt-1} + c \cdot [C]_{idz}^{idt-1} + b \cdot [C]_{idz+1}^{idt-1}$$

where $a = \frac{\Delta t}{2 \cdot \Delta z^2} \cdot (D_{sed\ idz} + D_{sed\ idz-1})$

$$b = \frac{\Delta t}{2 \cdot \Delta z^2} \cdot (D_{sed\ idz} + D_{sed\ idz+1})$$

and $c = 1 - a - b$

We consider that diffusion can not occur beyond the last section. The limit condition at this section is then written :

$$[C]_{Ndz}^{idt^*} = a \cdot [C]_{Ndz-1}^{idt-1} + (1-a) \cdot [C]_{Ndz}^{idt-1}$$

Resolution of the biogeochemical model

The resolution of the biogeochemical model is based, for all the species, on the following general form :

$$[C]_{idz}^{idt} = [C]_{idz}^{idt^*} + \Delta t \cdot \sum_R \alpha(C,R) \cdot V_R *$$

where V_R^* are the reaction rates calculated from the concentrations provided by the previous step and noted * and α(C,R) are the stoichiometric coefficients of the species C in the reaction R.

For iron and manganese oxides, the model is applied to the total concentrations given by :

$$[Fe(OH)_3]_{T\,idz}^{idt^*} = [Fe(OH)_3]_{C\,idz}^{idt^*} \cdot n_{idz} + [Fe(OH)_3]_{P\,idz}^{idt^*} \cdot (1 - n_{idz}) \cdot \rho_{sed}$$

$$[MnO_2]_{T\,idz}^{idt^*} = [MnO_2]_{C\,idz}^{idt^*} \cdot n_{idz} + [MnO_2]_{P\,idz}^{idt^*} \cdot (1 - n_{idz}) \cdot \rho_{sed}$$

After resolution, the concentrations of the particulate and colloidal forms of these oxides are obtained by admitting the conservation of their ratio :

$$[Fe(OH)_3]_{C\,idz}^{idt} = \frac{[Fe(OH)_3]_{C\,idz}^{idt^*}}{[Fe(OH)_3]_{T\,idz}^{idt^*}} \cdot [Fe(OH)_3]_{T\,idz}^{idt}$$

and $[Fe(OH)_3]_{P\,idz}^{idt} = \frac{[Fe(OH)_3]_{P\,idz}^{idt^*}}{[Fe(OH)_3]_{T\,idz}^{idt^*}} \cdot [Fe(OH)_3]_{T\,idz}^{idt}$

$$[MnO_2]_{C\,idz}^{idt} = \frac{[MnO_2]_{C\,idz}^{idt^*}}{[MnO_2]_{T\,idz}^{idt^*}} \cdot [MnO_2]_{T\,idz}^{idt} \text{ and } [Mn$$

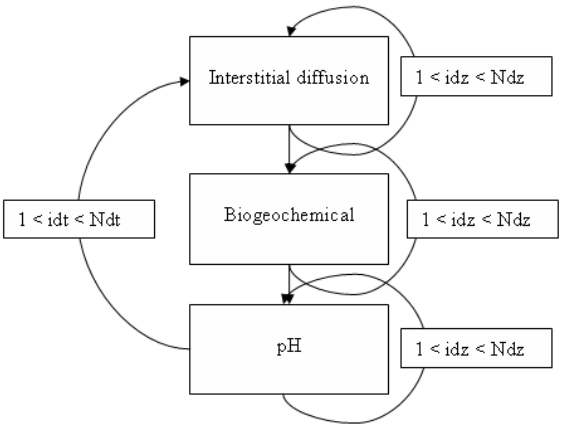

Fig.2. Main steps of the method of resolution

and $[MnO_2]_{P\,idz}^{idt} = \frac{[MnO_2]_{P\,idz}^{idt^*}}{[MnO_2]_{T\,idz}^{idt^*}} \cdot [MnO_2]_{T\,idz}^{idt}$

Resolution of pH

This resolution constitutes the end of the procedure. For each temporal and spatial step, the determination of the proton concentrations is found by setting F([H+]) to zero.

$$F([H^+]_{D\,idz}^{idt}) = [H^+]_{D\,idz}^{idt} - \left\{ \frac{Kc_1 \cdot (2 \cdot Kc_2 + [H^+]_{D\,idz}^{idt})}{[H^+]_{D\,idz}^{idt\,2} + Kc_1 \cdot [H^+]_{D\,idz}^{idt} + Kc_1 \cdot Kc_2} \cdot [\Sigma CO_3]_{D\,idz}^{idt} + \frac{Ks_1}{[H^+]_{D\,idz}^{idt} + Ks_1} \cdot [\Sigma H_2S]_{D\,idz}^{idt} + \frac{[H^+]_{D\,idz}^{idt} + 2 \cdot Kp_2}{[H^+]_{D\,idz}^{idt} + Kp_2} \cdot [\Sigma PO_4]_{D\,idz}^{idt} + \frac{Ke}{[H^+]_{D\,idz}^{idt}} - \frac{[H^+]_{D\,idz}^{idt}}{[H^+]_{D\,idz}^{idt} + Kn} \cdot [\Sigma NH_3]_{D\,idz}^{idt} + E_{idz}^{idt} \right\}$$

where $E_{idz}^{idt} = -2 \cdot [Ca^{2+}]_{D\,idz}^{idt} - 2 \cdot [Fe^{2+}]_{D\,idz}^{idt} - 2 \cdot [Mn^{2+}]_{D\,idz}^{idt} + 2 \cdot [SO_4^{2-}]_{D\,idz}^{idt} + [NO_3^-]_{D\,idz}^{idt} + [Cl^-]_{D\,idz}^{idt}$

The solution is obtained by applying the iterative method of Newton initialized by :

$$[H^+]_{D\,idz}^{idt,0} = [H^+]_{D\,idz}^{idt^*}$$

The function, $[H^+]_{D\,idz}^{idt,k+1} = [H^+]_{D\,idz}^{idt,k-1} - \frac{F([H^+]_{D\,idz}^{idt,k-1})}{\frac{\partial F([H^+]_{D\,idz}^{idt,k-1})}{\partial [H^+]_D}}$,

is then iterated while $F([H^+]_{D\,idz}^{idt,k}) > \varepsilon$. The retained value is thus obtained when this last condition is not met.

Analytical protocol

The modelling previously described is applied to vertical distributions of physicochemical parameters in natural sediment cores obtained by the following analytical protocol (Fig. 3) :

1) sampling of natural sediment cores,

2) analysis of the vertical profiles of chemical parameters (pH, redox, O_2),

3) vertical sectioning and separation between pore water and solid matter.

4) On each sub sectioned sample:

1. chemical analysis of each phase: organic matter, nutrients and metal content.

2. physical analysis: grain size, solid matter density, water content and porosity.

For purposes of clarity, we limit the presentation of analytical results to profiles of O_2, which initiates the biogeochemical processes and pH, which integrate all the processed considered. O_2 and pH measurements were made with Unisense microsensors every 0,2 cm for the first 2 centimetres and every 0,5 cm thereafter.

For dissolved O_2, the Unisense oxygen microsensor is a miniaturized Clark-type sensor with an internal reference and a guard cathode. The sensor is connected to a high-sensitivity picoammeter such as the Unisense PA200. Driven by the external partial pressure, oxygen from the environment penetrates the sensor tip membrane and is reduced at the gold cathode surface. The picoammeter converts the resulting reduction current into a signal, which is converted into a dissolved O_2 concentration equivalent (Garcia & Gordon 1992).

The Unisense pH microelectrodes are miniaturized glass electrodes. When the electrode tip is immersed in an aqueous solution and connected via a high-impedance millivoltmeter to a reference electrode immersed in the same solution, the pH electrode tip develops an electric potential relative to the reference electrode, which reflects the acidity of the solution.

Fig.1 describes the analysis performed to obtain the other physicochemical parameters and nutrients.

Application on natural sediments

In this section we present an application of this approach (analysis and modelling) to sediment cores collected near Beaumont de Pertuis in the Durance River (south of France) in July and November 2007. For these applications, we consider only the first 8 to 10 cm of the sediment cores, which are represented as discrete section of 0.1 cm depth. The time step is adjusted to ensure numerical stability. We suppose that the vertical distributions of the different parameters measured in the cores correspond to steady state conditions. The calculations are then performed until a steady state is reached and model results are finally compared to analytical results.

The initial and limit conditions should be representative of the long term exchanges between the sediment and the water column (deposition, erosion, diffusion, etc). As this information is not available, we assume an equilibrium state at the sediment-water interface so the initial and limit conditions are assumed to be constant and equal to the measurements done on the first layer of the core (table 6).

Table 6. Initial and limit conditions

Parameters		Sampling date July 2007	Sampling date November 2007
$[POM]_P$	(10^{-6} mol.g^{-1})	1500	1200
$[O_2]_D$	(10^{-6} mol.l^{-1})	185	115
$[NO_3^-]_D$	(10^{-6} mol.l^{-1})	95	400
$[MnO_2]_T$	(10^{-6} mol.l^{-1})	16	12
$[Fe(OH)_3]_T$	(10^{-6} mol.l^{-1})	380	700
$[SO_4^{2-}]_D$	(10^{-6} mol.l^{-1})	340	1000
$[Mn^{2+}]_D$	(10^{-6} mol.l^{-1})	0,1	0,8
$[Fe^{2+}]_D$	(10^{-6} mol.l^{-1})	200	60
$[\Sigma H_2S]_D$	(10^{-6} mol.l^{-1})	0	0
$[FeS]_P(z,t)$	(10^{-6} mol.g^{-1})	0	0
$[FeS_2]_P$	(10^{-6} mol.g^{-1})	0	0
$[NH_4^+]_D$	(10^{-6} mol.l^{-1})	0	0
$[\Sigma CO_3]_D$	(10^{-6} mol.l^{-1})	600	550
$[\Sigma PO_4]_D$	(10^{-6} mol.l^{-1})	0	0
$[MnCO_3]_P$	(10^{-6} mol.g^{-1})	0	0
$[FeCO_3]_P$	(10^{-6} mol.g^{-1})	0	0
$[Calcite]_P$	(10^{-6} mol.g^{-1})	250	250
$[Ca^{2+}]_D$	(10^{-6} mol.l^{-1})	480	850
pH		8	7.8

Dissolved oxygen profiles

The analytical profiles (Fig. 4) show that concentrations of dissolved O_2 decrease strongly within the first millimetres of the sediment column, becoming totally

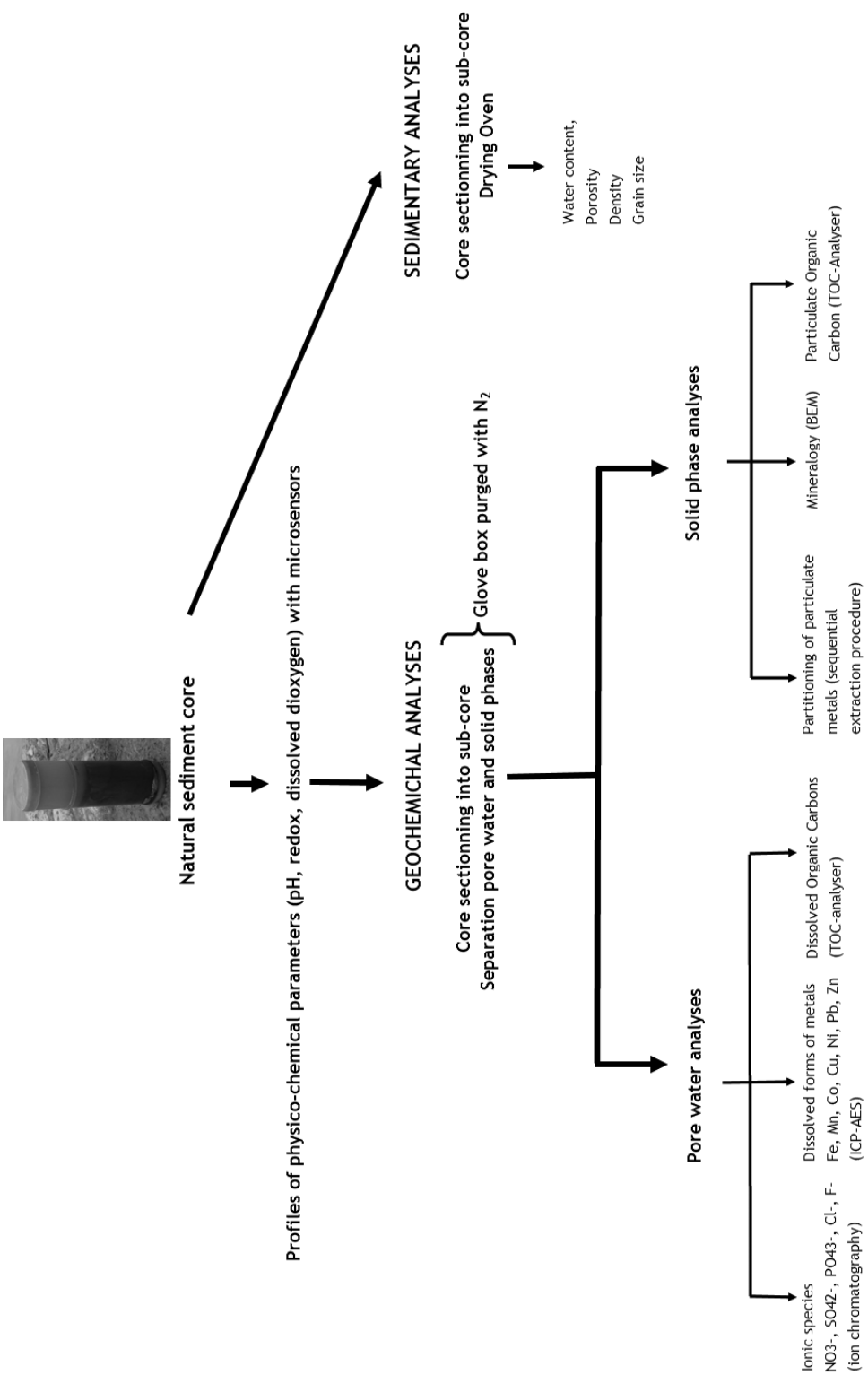

Fig. 3. Experimental protocol

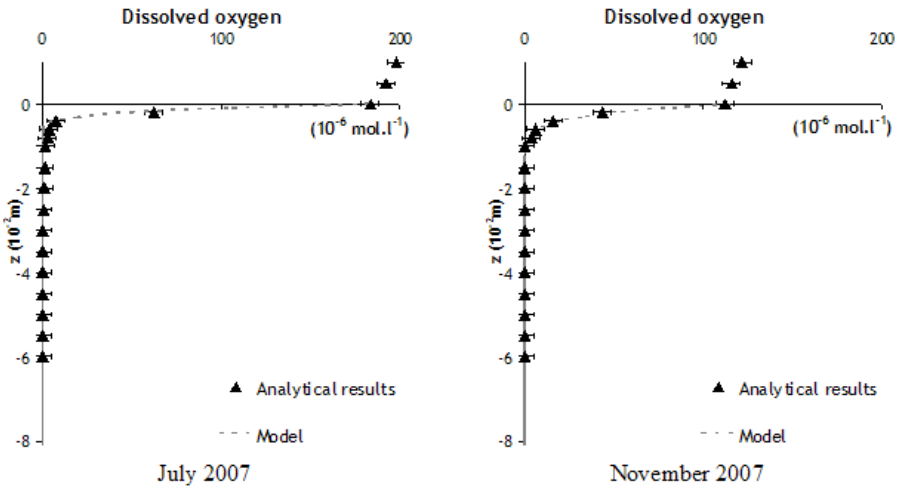

Fig. 4. Profiles of dissolved oxygen

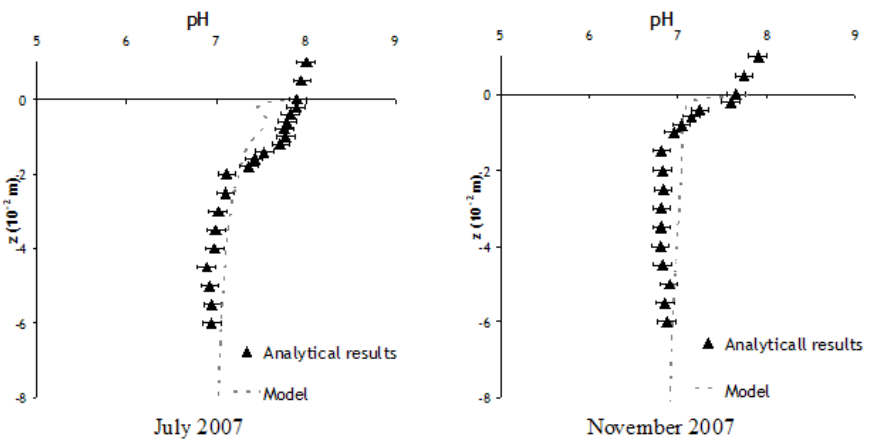

Fig. 5. Profiles of pH

anoxic at 1 centimetre of depth. The model attributes this decrease to bacterial aerobic respiration and allows for the determination of the organic matter mineralization constants. We observe that the values of these constants are higher in July 2007 than in November 2007, suggesting that the mineralization of organic matter by the biological activity is faster in warmer temperatures. Moreover, this is accentuated by the increase of particulate organic matter fluxes observed in July. Several authors (Hartog 2003, Serve et al. 1999) have confirmed such an increase in the production of particulate organic matter (planktons, algae, etc) and of an increased degradation by bacterial activity in summer. This result emphasises the effect of the seasonal variations of bacterial activity on the biogeochemical functioning of the sediments.

pH profiles

The pH profiles show a slight decrease (Fig. 5), with the maximal variation of one pH unit over the entire sedimentary column. The greatest decrease occurred within the uppermost 2 centimetres of the sediment, below which pH variation becomes negligible. In this depth interval, pH variations depend mainly on oxygen behaviour, which is totally consumed by aerobic respiration. This reaction produces H^+ ions, decreasing the porewater pH. Moreover, other biogeochemical reactions such as nitrate and sulphate reduction or oxidation by O_2 take place at this depth interval, also contributing to the production of H^+ ions. The only biogeochemical reactions responsible for the consumption of H^+ ions are calcite dissolution and manganese and iron oxide reduction (table 5).
The biogeochemical kinetic constants obtained by fitting the model on the analytical profiles are well within the range of values found in the literature (table 7), highlighting the complementarity of the analytical and modelling approaches to analyse and understand the functioning of the sediments.

Conclusions

This paper presents an approach coupling modelling and analytical protocols in order to analyse the vertical profiles of physico-chemical parameters in sedimentary columns of freshwater systems. The modelling approach links bio-geochemical processes (VanCappellen & Wang 1997) and interstitial diffusion (Boudreau 1996a, Boudreau 1996b). Unique to this approach is the determination of pH which extends and complements existing models. At the same time, we have developed an analytical protocol to obtain the vertical profiles of the main physicochemical parameters of natural sediment cores. To illustrate this approach, we present two applications in sediment cores sampled in July and November 2007 in the Durance, a river in the south of France. These applications show that the model and the analytical protocol allow to analyse and to understand the biogeochemical functioning of the sediments. In particular, the O_2 and pH profiles are correctly represented by the model.

This approach will be completed to analyse the behaviour of trace metals along the sedimentary column in view to guide management efforts to improve water quality and ecosystem health of current waters. To this end, the model could be linked to any water quality model to examine the effects of biogeochemical

Table 7. Kinetic parameters fitted

Kinetic constants	Sampling date : July 2007	Sampling date : November 2007
k_{Min} (s^{-1})	2.10^{-8}	2.10^{-9}
$k_{Li}^{O_2}$ (10^{-6} mol.l^{-1})	10	10
$k_{Li}^{NO_3^-}$ (10^{-6} mol.l^{-1})	40000	30
$k_{Li}^{MnO_2}$ (10^{-6} mol.l^{-1})	32	8
$k_{Li}^{Fe(OH)_3}$ (10^{-6} mol.l^{-1})	8	200
$k_{Li}^{SO_4^{2-}}$ (10^{-6} mol.l^{-1})	200	200
$k_{In,D}^{O_2}$ (10^{-6} mol.l^{-1})	30	10
$k_{In,[MOR,IOR,SR]}^{O_2}$ (10^{-6} mol.l^{-1})	30	10
$k_{In}^{NO_3^-}$ (10^{-6} mol.l^{-1})	10	10
$k_{In}^{MnO_2}$ (10^{-6} mol.l^{-1})	8	8
$k_{In}^{Fe(OH)_3}$ (10^{-6} mol.l^{-1})	200	1260
k_{ISP}^{+} (10^{6} l.mol^{-1}.s^{-1})	$3{,}17.10^{-8}$	$3{,}17.10^{-8}$
k_{ISP}^{-} (s^{-1})	$3{,}20.10^{-11}$	$3{,}20.10^{-11}$
k_{MP}^{+} (10^{6} l.mol^{-1}.s^{-1})	$2{,}58.10^{-6}$	$1{,}26.10^{-5}$
k_{MP}^{-} (s^{-1})	$2{,}58.10^{-10}$	$2{,}58.10^{-10}$
k_{IP}^{+} (10^{6} l.mol^{-1}.s^{-1})	$1{,}93.10^{-6}$	$1{,}29.10^{-6}$
k_{IP}^{-} (s^{-1})	$1{,}61.10^{-10}$	$1{,}61.10^{-10}$
k_{CP}^{+} (10^{6} l.mol^{-1}.s^{-1})	$3{,}80.10^{-8}$	$3{,}17.10^{-6}$
k_{CP}^{-} (s^{-1})	$1{,}61.10^{-10}$	$1{,}61.10^{-10}$
k_{PP} (10^{6} l.mol^{-1}.s^{-1})	$1{,}09.10^{-10}$	$1{,}09.10^{-10}$
k_{N} (10^{6} l.mol^{-1}.s^{-1})	$5{,}40.10^{-8}$	$5{,}40.10^{-8}$
k_{MO} (10^{6} l.mol^{-1}.s^{-1})	$3{,}49.10^{-8}$	$3{,}49.10^{-8}$
k_{IO} (10^{6} l.mol^{-1}.s^{-1})	$6{,}34.10^{-8}$	$6{,}34.10^{-8}$
k_{SO} (10^{6} l.mol^{-1}.s^{-11})	$3{,}54.10^{-8}$	$3{,}54.10^{-8}$

processes on the water and sedimentary column composition, particularly in terms of nitrates, phosphates and sulphates, the main nutrients responsible for the eutrophication of freshwater systems.

Acknowledgement

The authors gratefully thank Mr Laurent Vassalo for conducting the ICP-AES measurements and Ms Teresa Mathews for her review. Financial support for this research was provided by IRSN (Institut de Radioprotection et de Sureté Nucléaire) and the CNRS National Network ERICHE (Evaluer et Réduire l'Impact de la CHimie sur l'Environnement).

References

Adler M., Hensen C., Wenzhofer F., Pfeifer K. & Schulz H.D. 2001. - Modeling of calcite dissolution by oxic respiration in suprasoclinal deep-sea sediments, *Mar. Geol*., 177, 167-189.

Berg P., Rysgaard S. & Thamdrup B. 2003. - Dynamic modeling of early diagenesis and nutrient cycling. A case study in an arctic marine sediment, *Am. J. Sci.*, 303, 905-955.

Berner R.A. 1980. - *Early diagenesis - A Theoretical Approach*. Princeton University Press Princeton, N.J., 241 p.

Boudreau B.P. 1996a. - The diffusive tortuosity of fine-grained unlithified sediments, *Geochim. Cosmochim. Ac.*, 60, 3139-3142.

Boudreau B.P. 1996b. - A method-of-lines code for carbon and nutrient diagenesis in aquatic sediments, *Comput. Geosci.*, 22, 479-496.

Boudreau B.P. 1997. *Diagenetic Models and Their Implementation - Modelling Transport and Reactions in Aquatic Sediments* -, Verlag Berlin Heidelberg New York, 414 p.

Boudreau B.P. 1999. - Metals and models: Diagenetic modelling in freshwater lacustrine sediments, *J. Paleolimnol.*, 22, 227-251.

Canavan R.W. 2006. *Biogeochemical cycling of nutrients and trace metals in the sediments of Haringvliet Lake: response to salinization*, Universiteit Utrecht, 159 pp.

Canavan R.W., VanCappellen P., Zwolsman J.J.G., VandenBerg G.A. & Slomp C.P. 2007. Geochemistry of trace metals in a fresh water sediment: Field results and diagenetic modeling, *Sci. Total Environ.* 381, 263-279.

Forstner U. & Wittmann G.T.W. 1981. - *Metal pollution in the aquatic environment*. Springer-Verlag, Belin Heidelberg New York, 486 p.

Froelich P.N., Klinkhammer G.P., Bender M.L., Luedtke N.A., Heath G.R., Cullen D., Dauphin P., Hammond B. & Maynard V. 1979. - Early oxidation of organic matter in pelagic sediments of eastern equatorial Atlantic: Suboxic diagenesis, *Geochim. Cosmochim. Ac.*, 43, 1075-1090.

Garcia H.E. & Gordon L.I. 1992. - Oxygen solubility in seawater: Better fitting equations, *Limnol. Ocean.*, 37, 1307-1312.

Gutjahr A., Dabringhaus H. & Lacmann R. 1996a. - Studies of the growth and dissolution kinetics of the $CaCO_3$ polymorphs calcite and aragonite II. The influence of divalent cation additives on the growth and dissolution rates, *J. Cryst. Growth*, 158, 310-315.

Gutjahr A., Dabrinhaus H. & Lacman R. 1996b. - Studies of the growth and dissolution of $CaCO_3$ polymorphs calcite and aragonite I. Growth and dissolution rates in water, *J. Cryst. Growth*, 158, 293-309.

Hartog N. 2003. *Reactivity of organic matter and other reductants in aquifer sediments*, Universiteit Utrecht, 179 pp.

Jahnke R.A., Craven D.B., McCorkle D.C. & Reimers C.E. 1997. - $CaCO_3$ dissolution in California continental margin sediments: the influence of organic matter remineralisation, *Geochim. Cosmochim. Ac.*, 61, 3587-3604.

Jourabchi P., VanCappellen P. & Regnier P. 2005. - Quantitative interpretation of pH distributions in aquatic sediments: a reaction-transport modeling approach, *Am. J. Sci.* 305, 919-956.

Middelburg J.J. & Soetaert K. 2005. - The role of sediments in shelf ecosystem dynamics. pages 353-374 in *Chapter 13 : The Sea*. Harvard University Press (eds.).

Rickard D. 1997. - Kinetics of pyrite formation by the HS oxidation of iron(III) monosulfide in aqueous solutions between 25 and 125°C: The rate equation, *Geochim. Cosmochim. Ac.*, 61:135-147

Rickard D. 2006. - The solubility of FeS, *Geochim. Cosmochim.Ac.*, 70, 5779-5789.

Rickard D. & Luther III G.W. 1997. - Kinetics of pyrite formation by the HS oxidation of iron(III) monosulfide in aqueous solutions between 25 and 125°C: The mechanism, *Geochim. Cosmochim. Ac.*, 61,135-147.

Serve L., Gadel F., LLiberia J.-L. & Blazi J.-L. 1999. - Caractères biogéochimiques de la matière organique dans la colonne d'eau et les sédiments d'un écosystème saumâtre: l'étang de Thau-Variations saisonnières, *Rev. Sci. eau*, 12, 619-642.

Sigg L., Behra P. & Stumm W. 2001. - *Chimie des milieux aquatiques: chimie des eaux naturelles et des interfaces dans l'environnement*. Dunod, Paris, 567 p.

Soetaert K., Herman P.M.J. & Middelburg J.J. 1996. - A model of early diagenetic processes from the shelf to abyssal depths, *Geochim. Cosmochim. Ac.*, 60, 1019-1040.

Soetaert K., Hofmann A.F., Middelburg J.J., Meysman F.J.R. & Greenwood J. 2007. The effect of biogeochemical processes on pH, *Mar. Chem.* 105, 30-51.

Tromp T.K., Van Cappellen P. & Key R.M. 1995. - A global model for the early diagenesis of organic carbon and organic phosphorus in marine sediments, *Geochim. Cosmochim. Ac.*, 59, 1259-1284.

Van Capellen P. & Wang Y. 1997. - Reactive transport modeling of redox chemistry in aquatic sediments: implications for trace metal distributions, *ACS Div. Environ. Chem.*, 37, 134-136.

Wang Y. & VanCappellen P. 1996. - A multicomponent reactive transport model of early diagenesis: Application to redox cycling in coastal marine sediments, *Geochim. Cosmochim. Ac.*, 60, 2993-3014.

Wijsman J.W.M. 2001. - *Early diagenetic processes in northwestern Black Sea sediments*, Netherlands Institute of Ecology (University Groningen), Centre for Estuarine and Coastal Ecology, 121 p.

Wijsman J.W.M., Herman P.M.J., Middelburg J.J. & Soetaert, K. 2002. - A Model for Early Diagenetic Processes in Sediments of Continental Shelf of Black Sea, *Estuarine Coast. Shelf Sci.*, 54, 403-421.